VIGIL: A Python tool for automatized probabilistic VolcanIc Gas dIspersion modeLling

Fabio Dioguardi[*,1], Silvia Massaro[2,3], Giovanni Chiodini[3],
Antonio Costa[3], Arnau Folch[4], Giovanni Macedonio[5],
Laura Sandri[3], Jacopo Selva[3], Giancarlo Tamburello[3]

[(1)] British Geological Survey, The Lyell Centre, Edinburgh, United Kingdom

[(2)] Dipartimento di Scienze della Terra e Geoambientali, Università degli Studi "Aldo Moro", Via E. Orabona 4, 70125, Bari, Italy

[(3)] Istituto Nazionale di Geofisica e Vulcanologia, Sezione di Bologna, Via D. Creti 12, 40128, Bologna, Italy

[(4)] Geociencias Barcelona (GEO3BCN-CSIC), Barcelona, Spain

[(5)] Istituto Nazionale di Geofisica e Vulcanologia, Osservatorio Vesuviano, Via Diocleziano 328, 80124, Napoli, Italy

Abstract

Probabilistic volcanic hazard assessment is a standard methodology based on running a deterministic hazard quantification tool multiple times to explore the full range of uncertainty in the input parameters and boundary conditions, in order to probabilistically quantify the variability of outputs accounting for such uncertainties. Nowadays, different volcanic hazards are quantified by means of this approach. Among these, volcanic gas emission is particularly relevant given the threat posed to human health if concentrations and exposure times exceed certain thresholds. There are different types of gas emissions but two main scenarios can be recognized: hot buoyant gas emissions from fumaroles and the ground and dense gas emissions feeding density currents that can occur, e.g., in limnic eruptions.

Simulation tools are available to model the evolution of critical gas concentrations over an area of interest. Moreover, in order to perform probabilistic hazard assessments of volcanic gases, simulations should account for the natural variability associated to aspects such as seasonal and daily wind conditions, localized or diffuse source locations, and gas fluxes.

Here we present VIGIL (automatized probabilistic VolcanIc Gas dIspersion modeLling), a new Python tool designed for managing the entire simulation workflow involved in single and probabilistic applications of gas dispersion modelling. VIGIL is able to manage the whole process from meteorological data processing, needed to run gas dispersion in both the dilute and dense gas flow scenarios, to the post processing of models' outputs. Two application examples are presented to show some of the modelling capabilities offered by VIGIL.

Key words: Atmospheric gas dispersion; Volcanic gases; Python workflow; Diagnostic wind model; Probabilistic volcanic hazard assessment

1. Introduction

The injection of volcanic gases in the atmosphere can be very hazardous to life and global environment. While the impacts from large volcanic eruptions have been widely studied [e.g. Grattan and Pyatt, 1994; Parker et al., 1996; Self, 2006], the lower atmospheric boundary layer gas dispersion from persistently degassing volcanoes or particular tectonic areas also deserves attention since it can have an important effect on the regional and global environment [e.g., Williams-Jones and Rymer, 2015]. Volcanic gas hazard is mainly related to the reaching of hazardous concentration levels in the air of some species that are dangerous for human health and life for relatively long-time exposures (e.g. CO_2, H_2S and SO_2) or even a mixture of such species [e.g., IVHHN, 2005]. Figure 1a shows the range of gas hazards and the scale of their impacts [Edmonds et al., 2018]. Long-term exposure to volcanic gas, aerosol and particulate matter can produce acidification of soil, pollution of water, impinge on livestock and fisheries [Cronin and Sharp, 2002]. Volcanic gases may be passively transported by wind (e.g. fumaroles; Figure 1b) or may accumulate far from their source flowing down valleys as a gravity flow, engulfing and asphyxiating people [e.g. Costa and Macedonio, 2016; Folch et al., 2017; Figure 1c]. For these reasons, the evaluation of gas hazard should be part of any multi-hazard evaluation in volcanic environments [e.g. Selva et al., 2020].
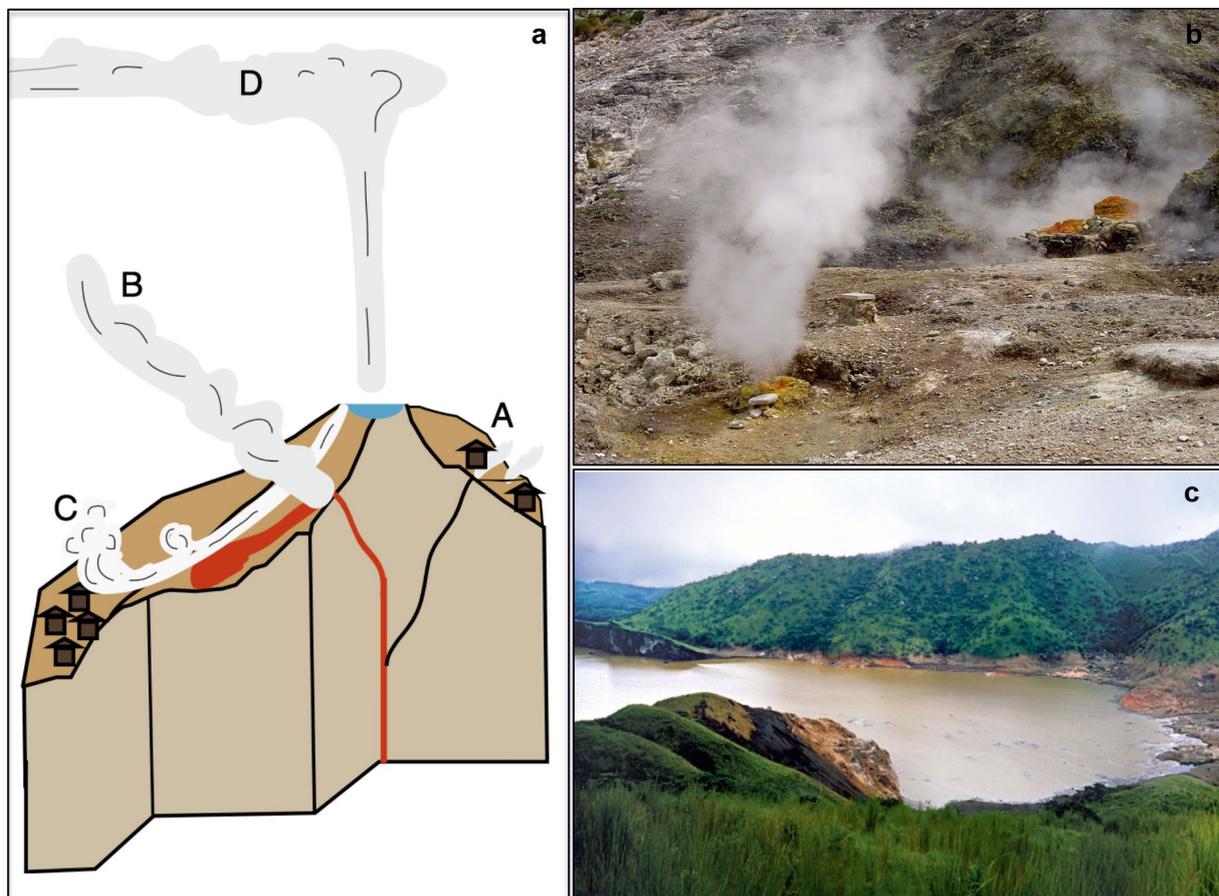
Figure 1. a) Cartoon showing different types of gas dispersion: (A) diffuse degassing through fractures and faults; (B) acidic tropospheric plumes from active volcanic vents that may persist for many years during non-eruptive activity at some volcanoes; (C) sudden flows of cold CO_2-rich gases occurring as a consequence of lake overturn or phreatic explosions; (D) large explosive eruptions inject acid gases directly into the upper troposphere or stratosphere (from Edmonds et al., 2018; Creative Commons Attribution 4.0 International License: https://creativecommons.org/licenses/by/4.0/); b) Example of passive degassing from Solfatara crater, Campi Flegrei (from Wikipedia; https://it.wikipedia.org/wiki/File:Solfatara_Krater.JPG); c) Example of Lake Nyos in 1986 which, after a large limnic eruption, flooded the surrounding area with gases denser than air (from Wikipedia; https://upload.wikimedia.org/wikipedia/commons/8/8c/Tml15-16_Nc.jpg).

The dispersion of gases generated from volcanoes and Earth degassing can be simulated by solving the complete set of conservation equations for mass, momentum, and energy. However, this approach is computationally expensive, since it requires three-dimensional computational fluid dynamics models [e.g. Cortis and Oldenburg, 2009; Macedonio and Costa, 2002]. In a probabilistic hazard context requiring numerous simulations, simplified gas transport models are commonly used to strongly reduce the computational cost [e.g., by using single species of gas, assuming the gas as incompressible; Costa and Macedonio, 2016]. Numerical modelling of both heavy [e.g. Burton et al. 2016; Costa et al., 2008; Folch et al., 2009, 2017] and light gases [e.g. Chiodini et al., 2010; Costa et al., 2005; Granieri et al., 2013; Pedone et al., 2017] accounts for topographic effects, variation of atmospheric conditions and wind directions. For a gas denser than air, the flow behaviour over complex topography is generally described using depth-averaged variables [shallow layer approach, e.g. Hankin and Britter, 1999], while for dispersion of a diluted gas passively driven by wind advection and atmospheric turbulence, simpler advection-diffusion equations are considered [e.g. Prabha and Mursch-Radlgruber, 1999] to make the problem computationally lighter [Costa and Macedonio, 2016]. Alternative methodologies consisting in simulating the spread and dispersal of gases in a numerical weather prediction model have also been proposed [e.g. Burton et al., 2016].

In this study, we use two open-source codes for modelling dilute and dense gas dispersion, respectively: DISGAS v.2.2.4 [hereafter referred to as DISGAS; Costa et al., 2005; Costa and Macedonio, 2016; http://datasim.ov.ingv.it/ models/disgas.html] and TWODEE-2 v.2.6 [hereafter referred to as TWODEE; Folch et al., 2009; 2017; Hankin and Britter, 1999; http://datasim.ov.ingv.it/models/twodee.html]. Both models are written in Fortran and need a terrain-following mass-consistent wind model (i.e. that ensures mass conservation), such as the Diagnostic Wind Model [DIAGNO v.1.1.6, hereafter referred to as DIAGNO; Douglas et al., 1990; http://datasim.ov.ingv.it/models/diagno. html]. DISGAS reproduces the passive dispersion of a gaseous pollutant governed by wind and atmospheric turbulence. It yields gas concentrations (e.g., CO_2) expressed as values in excess of background gas species levels in the air at heights selected by the user in a terrain-following coordinate system. The model does not account for the chemical reactivity of components and also neglects gas solubility in condensing H_2O droplets. This, however, does not limit its application to the assessment of gas species dispersion, in light of the conservative behavior of this component [Pedone et al., 2017]. On the contrary, TWODEE simulates the heavy gas flow in a relatively calm ambient based on the shallow water equations for fluid depth, depth-averaged horizontal velocities and depth-averaged fluid density. It can be used for modelling gas dispersion near the ground over complex terrains [Folch et al., 2009; 2017].

In the last decades, probabilistic volcanic hazard assessment (PVHA) methodologies have allowed the quantification of intrinsic uncertainties relating to volcanic hazards, contributing to risk reduction strategies [e.g., Magill and Blong, 2005; Martí et al., 2008; Neri et al., 2008; Marzocchi et al., 2010; Selva et al., 2010; Sandri et al., 2014]. Computational models of volcanic gas dispersion have significantly advanced [e.g. Costa and Macedonio, 2016; Folch et al., 2009, 2017] and now represent a valuable tool to make quantitative gas dispersal evaluations that can be used to forecast potentially dangerous concentrations, study past events, quantify hazard and also understand the physic-chemical changes occurring in the magmatic feeding systems or in hydrothermal aquifers [i.e., Edmonds et al., 2018; Massaro et al., 2021]. Furthermore, they can be used to cross-validate measurements of gas emission rates [Massaro et al. 2022].

The use of such models in PVHA is based on multiple deterministic simulations of gas concentration in the area of interest aimed to explore not only the natural variability in input and boundary conditions (seasonal and daily wind variability, source position and gas flux at the emission sources), but also the impact of the uncertainty on other controlling factors such as, for example, the resolution of topographic data [Tierz et al., 2016; Selva et al., 2018; Massaro et al., 2021]. The underlying workflow motivated the development of VIGIL (automatized probabilistic VolcanIc Gas dIspersion modeLling), a new open-source tool written in Python and designed to control the complete workflow using DISGAS and TWODEE [Massaro et al., 2022]. VIGIL controls the execution of DIAGNO to generate time-dependent terrain-adapted wind fields from either user-provided data or retrieved by the Copernicus ERA5 reanalysis dataset [Copernicus Climate Change Service, 2017]. Then it runs DISGAS or TWODEE (or both) with different setup options available to the user and, finally, it processes the numerical outputs and produces graphical outputs. Each workflow stage can be run in parallel, hence significantly reducing the typical times required for running dispersion simulations in PVHA applications.

This manuscript is arranged as follows. In the first part we briefly review the numerical models DIAGNO, DISGAS, and TWODEE, then we present the VIGIL workflow (v1.2, https://github.com/BritishGeologicalSurvey/VIGIL/ releases/tag/v1.2) and its main functionalities. Finally, we discuss two application examples by running DISGAS (i.e. Solfatara crater, Campi Flegrei, Italy) and TWODEE (i.e. Mefite d'Ansanto area, Italy).

2. Methods

2.1 The modelling strategy

The atmospheric dispersion of a gas released from a given source is governed by the starting density contrast between the gas and the environment (atmospheric air) and turbulent entrainment, the latter controlled by lateral eddies that increase the mixing with air around the edges of the plume thereby decreasing its averaged density [e.g. Costa et al., 2005; Folch et al., 2009; Hankin and Britter, 1999]. Based on the starting buoyancy of the gas phase relative to the environment, which can be quantified by the reduced gravity ($g' = (\rho_g - \rho_e)/\rho_e$, where ρ_g and ρ_e are the gas and environment density, respectively), the source extension (which can be quantified by the plume radius at the source, r), the source gas flux (q) and the wind speed (v), which all determine the flow Richardson number Ri at the source:

$$Ri = \frac{1}{v^2}\left(\frac{g'q}{r}\right)^{\frac{2}{3}} \tag{1}$$

two regimes are possible [Cortis and Oldenburg, 2009; Costa et al., 2013]:
1. If $Ri < 0.25$, the gas transport is passive and dominated by the wind advection and diffusion (passive dispersion). We call this "light-gas" regime;
2. If $Ri > 1$, the gas transport is dominated by the density contrast between the gas and the surrounding environment; in this case the gas flows over the topography until the density contrast persists. We call this "heavy-gas" regime.

Although the atmospheric gas dispersion can be generally described by solving 3D equations for the conservation of mass, momentum, and energy for each gas specie, several scenario-specific simplifications are assumed to reduce the computational time [i.e., single species of gas, incompressible fluid; Costa and Macedonio, 2016], eventually approaching the two end-member scenarios represented by the DISGAS and TWODEE models. In both cases, the momentum coupling with the atmospheric air is taken into account by considering the wind field, which is the main factor controlling the light-gas dispersion of gases and one of the controlling factors (together with density contrast) in the heavy-gas case. Details on the wind model pre-processor (DIAGNO) and the two models used for the passive light-gas and for the heavy-gas dispersion (DISGAS and TWODEE) can be found in VIGIL User's Manual.

2.2 The VIGIL workflow

VIGIL is a set of three Python scripts designed to manage the whole workflow leading to gas dispersion simulation outputs, from meteorological data retrieval and processing to graphical output production. VIGIL works both in forecast and reanalysis mode, and allows simulations over long period of times in both modes.
It is executed in the workflow as shown in Figure 2:
– **weather.py**: depending on the simulation mode (forecast or reanalysis), it prepares the meteorological data by either retrieving forecast data from the NOAA-NCEP Global Forecast System (GFS) Numerical Weather Prediction (NWP) dataset (https://www.ncei.noaa.gov/products/weather-climate-models/global-forecast) or reanalysis data from the ECMWF ERA5 NWP dataset [Copernicus Climate Change Service, 2017]. User-provided data from local weather stations can also be used in reanalysis mode. NWP data, which are available on a global grid with horizontal resolution of 0.25° for ERA5 and 18 miles for GFS, are interpolated onto the computational domain specified in input by the user. In reanalysis mode, the script is designed to randomly sample N days from a time interval defined by the user. If data from a local weather station are available, the script extracts these data in the time interval specified by the user from selected data files. The N days can be processed in parallel as blocks of N_{proc} simultaneous processes specified by the user. Data are then organized in folders to be used by the meteorological processor DIAGNO.
– **run_models.py**: it runs DIAGNO and subsequently DISGAS or TWODEE. For each of the N simulations (days), the user can assess the gas emission sources within the computational domain by using random source locations (source locations are selected from a probability map) or by defined source locations (source locations

are read from a list containing its coordinates). In both cases, the number of sources can be fixed or randomly sampled from a range defined by the user. In the same way, the associated gas fluxes can be read from a list (fixed source emission) or randomly sampled by an Empirical Cumulative Distribution Function (ECDF) (random source emission), which is built by *run_models.py* based on data provided by the user in the file *flux.txt* (see below). A combination of fixed and random emissions is also possible. The *N* days can also be processed in parallel as blocks of N_{proc} simultaneous processes specified by the user.

– **post_process.py**: it reads the DISGAS or TWODEE outputs produced by *run_models.py* and converts the model outputs in concentration of other gas species (e.g., CO_2, H_2S) based on the gas species properties made available by the user in the file *gas_properties.csv*. Tracking points can be specified to track the time evolution of gas concentration at specific locations. In PVHA applications, the script merges the outputs of the *N* to build ECDF of the gas concentration and produces plots of the modelled concentrations at the user's specified exceedance probabilities ("probabilistic outputs" in Figure 2), time steps and vertical layers. If tracking points are active, hazard curves (plot of exceedance probability vs. gas concentrations) are automatically produced for the specified locations. Plots of the time-averaged concentrations can also be created via this script. Finally, all the graphical outputs can optionally display the topography layer as map background.
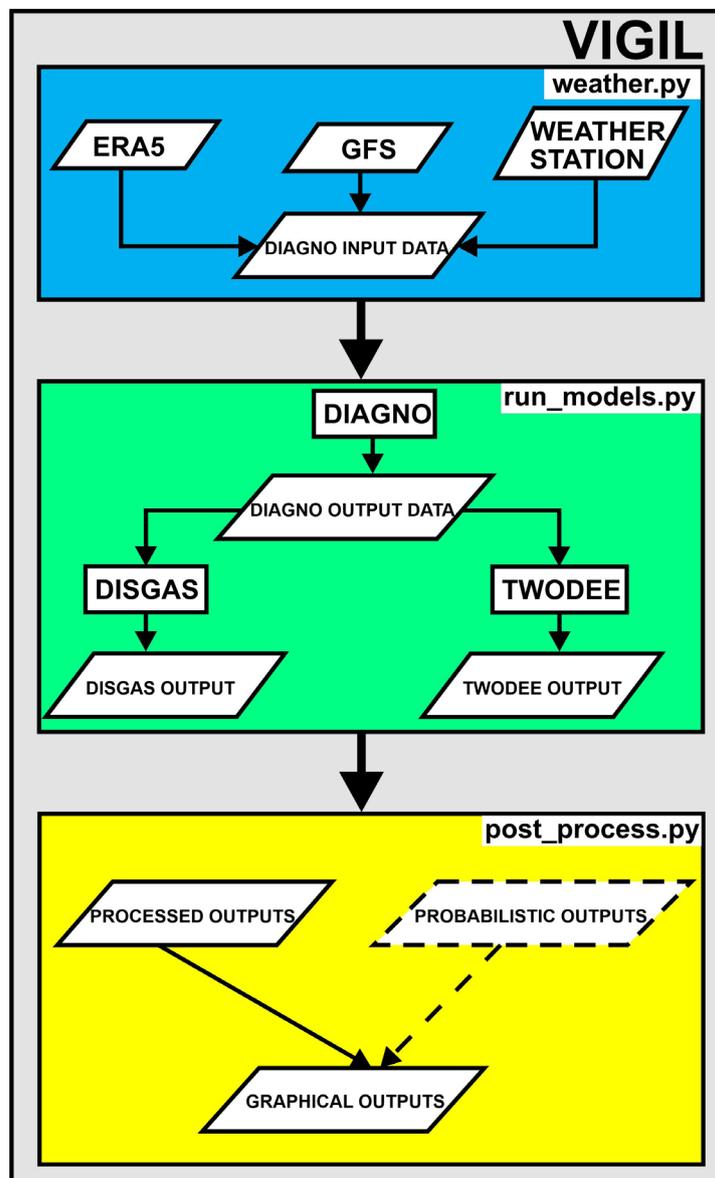

Figure 2. Simplified scheme of the VIGIL workflow.

To run VIGIL, the following files are mandatory:

– **diagno.inp**: it denotes the DIAGNO input file. This file has a fixed structure, which is explained in the DIAGNO user manual. Working versions can be found in the Example folders: the user can use any working version of the *diagno.inp* file from the example without modifying it. Then *weather.py* modifies all the necessary entries. It is essential that the user does not alter the structure of the reference file manually.

– **"modelname".inp**: it is the control file of DISGAS and/or TWODEE. *modelname* should be "disgas" or "twodee" depending on the model at stack. The user is referred to the DISGAS and TWODEE user manuals for details on the structure of these files. Similar to diagno.inp, the user can take any of the files in the Example folders; *run_models.py* will modify these files accordingly.

– **topography.grd**: a file that describes the topography in Golden Surfer v.6© GRD format following the format required by DISGAS and TWODEE.

– **roughness.grd**: a file that describes the terrain roughness height in Golden Surfer v.6© GRD format following the format required by DISGAS, in which it is also possible to set a uniform value in the disgas.inp file so that the roughness.grd is not required. The surface roughness height influences the vertical wind profile. Typical values range from about 10^{-5} m over an iced surface, 0.05 m over grass-covered soils up to 1 m or more over forest or urban areas.

Details on the GRD file structure are available in the DISGAS and TWODEE User Manuals.

Other optional files are required depending on the options chosen by the user. When weather data from local weather stations are used ("weather station" in Figure 2), these should be provided in separate files for each weather station stored into a "weather_stations" folder. In this case, the following input files are required:

– **weather_stations_list.txt**: it contains the list of files with the weather station data and that are stored in the folder "weather_stations". Mandatory only when the user runs DIAGNO with local meteorological data.

– **"file_name".txt**: it contains the meteorological data acquired by a weather station. The file has to be included in the "weather_station" folder. Mandatory only when the user runs DIAGNO with local meteorological data.

Further optional files can be provided to control the emission sources. These are:

– **flux.txt**: it contains a list (in a column) of possible values of the gas source emission rate (kg s^{-1}) that VIGIL uses to build an ECDF from which it randomly selects a user-defined number of possible values to be attributed to each source.

– **sources_input.txt**: a file that contains a list of fixed sources provided by the user. It is structured as in the following:

– **probability_map.grd**: a file that contains the probability that each cell in the hazard domain acts as a gas source location. It has the same format as the topography.grd and roughness.grd files (Golden Surfer v.6© GRD) and is a structured as a matrix with NY rows and NX columns, where NX and NY are the number of cells in the domain along the *x* and *y* directions, respectively. NX and NY must coincide with the values indicated in *modelname*.inp.

Furthermore, the file **gas_properties.csv** is used by *post_process.py* when the user needs to convert the concentration of the gas species tracked by TWODEE or DISGAS into the concentration of another gas species and when a conversion of the resulting concentration from kg m^{-3} to ppm or vice-versa is required. This option can be useful when an abundant gas species (e.g. H_2O) is set as the gas specie tracked in DISGAS and TWODEE and considered as carrier for less abundant non-reacting species (e.g. CO_2) [Massaro et al., 2021]. For this conversion, the molar ratio between the species (converted / original) and the molar weight of the new species in g mol^{-1} are needed. Note that it is possible to:

– provide more than one species. If more than one species is provided, all the columns with the molar ratios should be aligned to the left of the columns with the species molar weights;

– provide more than one value of molar ratio, which is suggested since this parameter is affected by a significant uncertainty. In this case, the routine *post_process.py* randomly selects one of the molar ratio values to be used for the conversion from an ECDF built by the code based on the data provided in the *gas_properties.csv* file.

Finally, the file **tracking_points.txt** is required by *post_process.py* when the tracking points option is activated by the user. The file lists the locations (in UTM coordinate) and elevations (in m above the ground) of the selected locations.

3. Results

In this section, two examples show part of the wide range of capabilities of VIGIL that can be used for different applications. The first example is referred to DISGAS, while the second shows an application of TWODEE. In particular, we will focus on the novelty introduced by the VIGIL, that is to generate hazard maps for gas hazard assessment purposes.

3.1 DISGAS application: Solfatara crater (Campi Flegrei, Italy)

This application is focused on the dispersal of CO_2 released from Solfatara crater (Campi Flegrei, Italy) and the hazard related to the intense soil diffusive degassing and fumarolic sources which has shown large variation in the last 20 years [Chiodini et al., 2021]. In this case, we selected a scenario typical of gas fluxes of about 10 years ago, setting an emission from soil diffuse degassing at 1000 t d^{-1} and at 490 t d^{-1} from fumarolic vents [Granieri et al., 2013; Pedone et al., 2014; Cardellini et al., 2017]. Temperatures of the gases emitted from Solfatara are
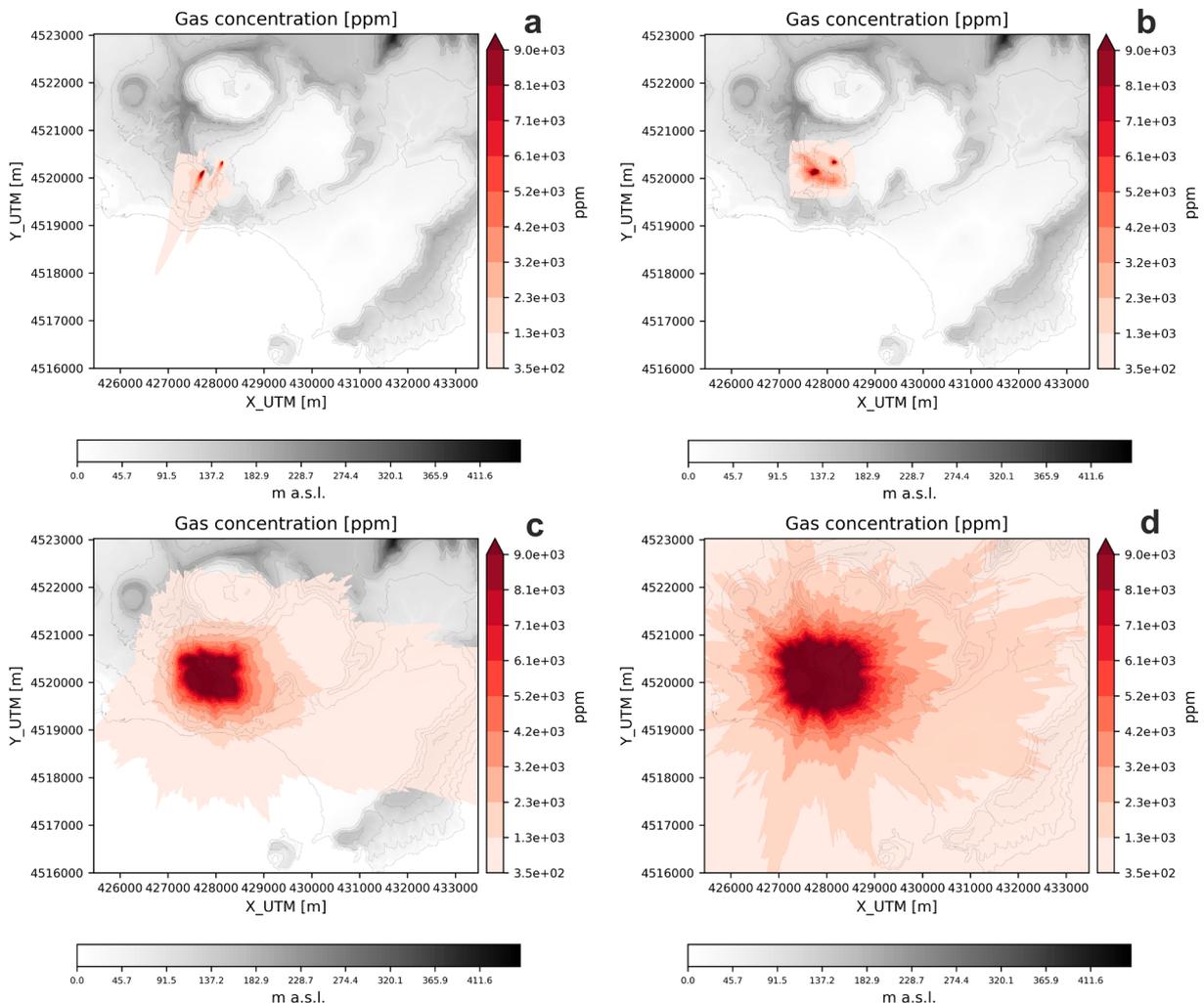
Figure 3. Probabilistic concentration maps of the Solfatara test case; CO_2 concentration (in ppm) is shown at 1.5 m above the ground after 24 hours. a) CO_2 concentration for one of the 100 days; b) CO_2 concentration corresponding to the 50% exceedance probability of the whole simulation dataset; c) CO_2 concentration corresponding to the 5% exceedance probability of the whole simulation dataset; d) CO_2 concentration corresponding to the 1% exceedance probability of the whole simulation dataset. We thank the Laboratory of Geomatics and Cartography of the Osservatorio Vesuviano – INGV, Naples, for providing the DEM of the Campi Flegrei area.

ca. 96-162 °C from fumaroles [Chiodini et al., 2001] while the flux weighted temperature of diffusing soil is 66 °C [Costa et al., 2005]. Such temperatures contribute to balance, directly at the source, the increase of gas density due to the greater molecular weight ($M_{CO2}/M_{air} = 44/29$). Moreover, typical surface wind velocities, intensity of the gas source, and size of the plume are such that $Ri < 0.25$ (see Section 2). For these conditions, the passive dispersion assumption is appropriate [Costa et al., 2005].

In this example, we run DIAGNO and DISGAS on a computational domain of 8,025 km × 7,025 km × 75 km with a horizontal resolution of 25 × 25 m, while the spacing of the vertical layers ranges from 0.5 m above the ground to 75 m towards the top of the computational domain. The topography is represented by a 1 m-resolution DEM. We use *weather.py* to randomly sample 1000 days from the period 1990-2020 and download meteorological data for these days from the ERA5 reanalysis dataset. Therefore, we run 1000 simulations with *run_models.py* using the fixed source locations of the active fumaroles, and also considering the CO_2 diffusive contribution on a gridded source [Cardellini et al., 2017], the latter reproduced by a set of equally-spaced sources (see *sources_input.txt* file in the example_1 folder of the Supplementary Material).

Figure 3 shows some of the outputs produced by *post_process.py* for this test case. Here, we represent the concentration in ppm on a fixed linear scale (350-10,000 ppm) and we display the topography layer. Specifically, we show: the CO_2 concentration for a single simulation (Figure 3a) considering exceedance probabilities of 50%, 5% and 1% (Figures 3b-c-d). All plots represent the concentration field at the last time step of the simulations (+24 hours from the beginning of the emission), at 1.5 m above the ground.

Figure 3 represents one of the capabilities of VIGIL, i.e. to analyze the meteorological variability in a framework of probabilistic simulations. At 50% exceedance probability (i.e., the most likely scenario; Figure 3b), the highest CO_2 concentrations are localized in the emission area. For smaller exceedance probability, we go towards less likely and more "worst-case" oriented scenarios (5% and 1% exceedance probabilities, Figures 3c-d). In these cases, the areas with the highest concentrations expand significantly and some tendency for preferential dispersion directions can be observed, which are likely related to the dominant wind pattern. The seasons play also a role, especially at mid-latitudes like in this application. The script *weather.py* allows the user to select specific years, months and days from the time period to sample. Therefore, it is possible to, e.g., select only days in winter by specifying December, January and February in the *weather.py* command.

Figure 4 displays an example of a hazard curve produced (exceedance probability vs. C [ppm]) at a location in the domain for the last time step of the simulation (+24 hours from the emission start) at 1.5 m above the ground.
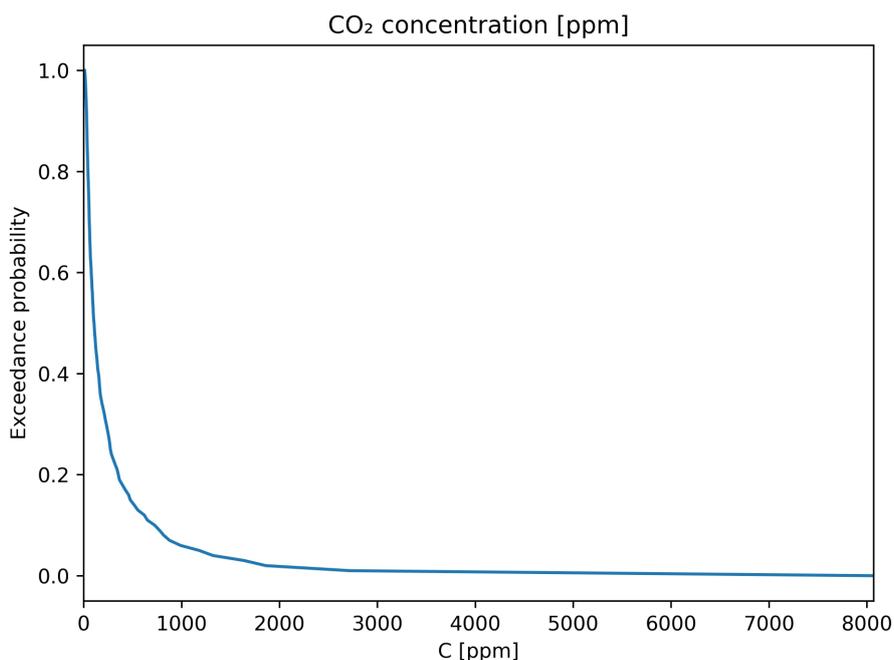

Figure 4. Hazard curve (Exceedance vs. C in ppm) for a selected location specified in the file *tracking_points.txt* at +24 hours from the emission start at 1.5 m above the ground.

All the input files, the VIGIL commands and the graphical outputs shown in this section are available in Supplementary Material 1. A more extensive analysis, considering the variability of the gas source and the persistency of concentrations in the air is the subject of an on-going study.

3.2 TWODEE application: the case of Mefite d'Ansanto (Italy)

Mefite d'Ansanto represents the largest natural emission of low temperature CO_2-rich gases from non-volcanic environment ever measured on Earth [Chiodini et al., 2010]. Under low-wind conditions, the gas flows along a narrow natural channel producing a persistent invisible gas river (see Figure 5), which has already killed three people in the 1990s and many other according to historical chronicles [Chiodini et al., 2010, Costa et al., 2008].
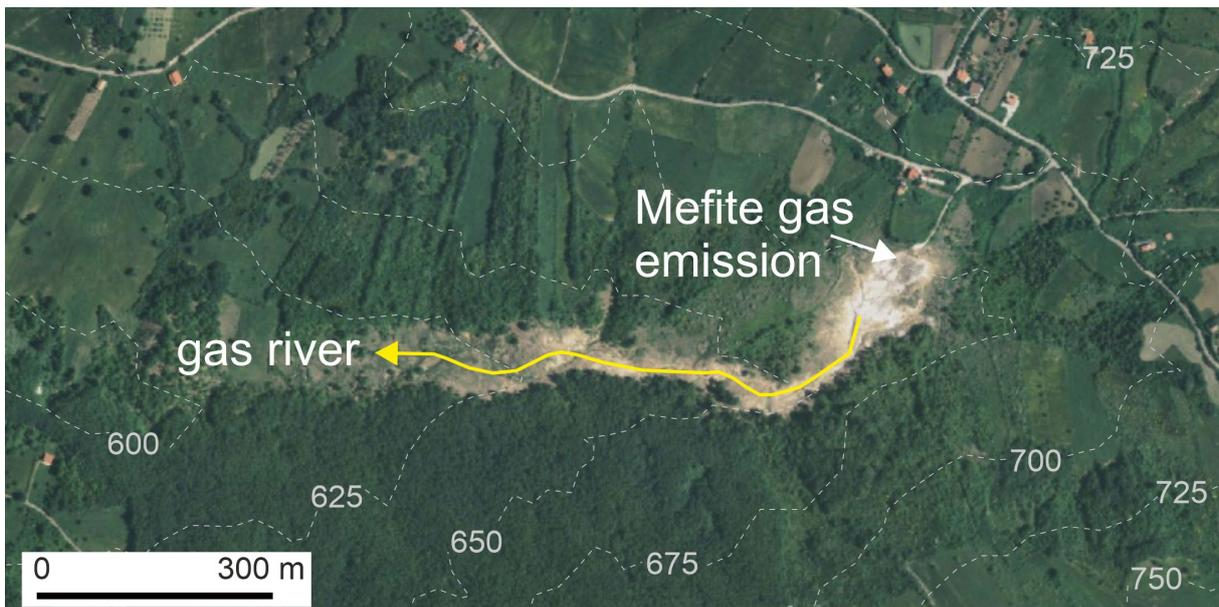
Figure 5. Aerial photo of the Mefite gas emission and the associated gas river (modified after Chiodini et al, 2010). Copyright 2010 by the American Geophysical Union.

Here, in order to reproduce the formation of the channelized gas river, we run DIAGNO and TWODEE on a computational rectangular domain of 1200×510 m with a horizontal resolution of 3×3 m. Concentration of the gas species is computed at seven levels, from 5 cm to 3 m above the ground. The topography is represented by an 8.9 m-resolution DEM modified after the 10 m-resolution DEM TINITALY/01 [Tarquini et al., 2007]. Similar to the previous example (section 4.1), we use *weather.py* to randomly sample 1000 days from the period 1990-2020 and download meteorological data for these days from the ERA5 reanalysis dataset. Therefore, we run 1000 simulations with *run_models.py*. The CO_2 is emitted from an area towards the east of the computational domain with an overall flux of 23.18 kg s^{-1} (2003.1 ton d^{-1}); this has been approximated by 48 dense gas sources all represented by squares of 10 m sides with a constant flow rate of 0.483 kg s^{-1} (see *sources_input.txt* file in the "example_2" folder of the Supplementary Material).

Figure 6 shows the outputs produced by *post_process.py*. Similar to the previous application, we represent the concentration in ppm on a fixed linear scale (350-10,000 ppm) displaying the topography layer. All plots are obtained by sampling the ECDF created by *post_process.py* from the 1000-days dataset at specific exceedance probabilities and vertical levels; furthermore, all plots refer to the concentration averaged over the whole simulation duration (2 hours). Specifically, we show: the CO_2 concentration at 0.05 m above the ground at 5% and 1% exceedance probability (Figures 6a-b); the CO_2 concentration at 2 m above the ground at 5% and 1% (Figures 5c-d) exceedance probability.
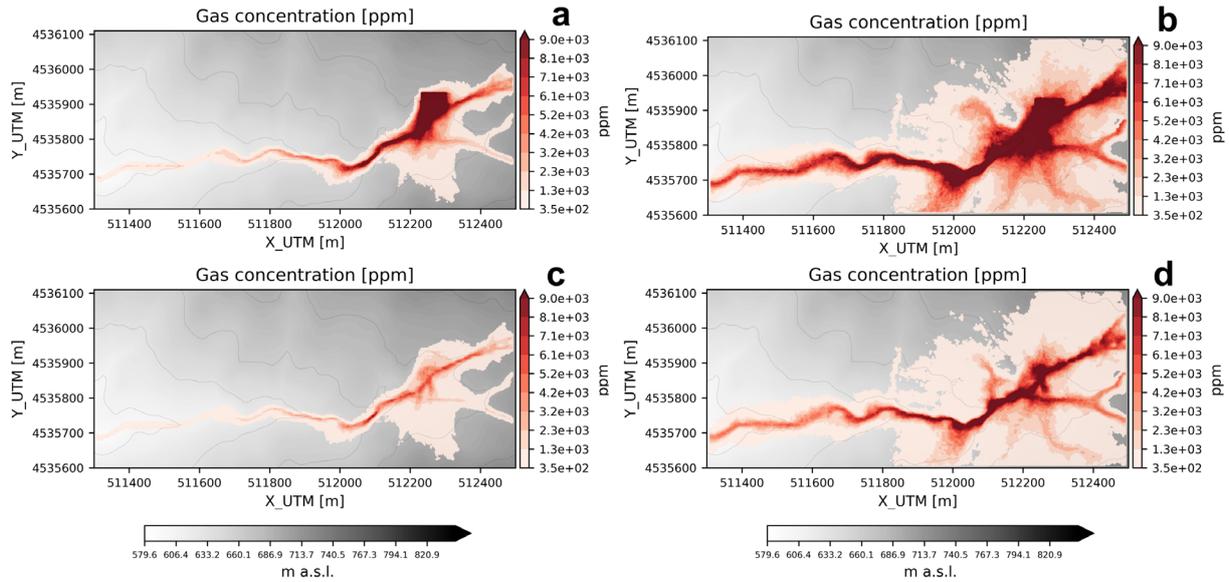
Figure 6. Probabilistic concentration maps of the Mefite d'Ansanto test case; all plots represent CO_2 concentration (in ppm) obtained by sampling the ECDF built on the 1000-simulations dataset at user-requested exceedance probabilities. a) CO_2 concentration at 0.05 m above the ground corresponding to the 5% exceedance probability; b) CO_2 concentration at 0.05 m above the ground corresponding to the 1% exceedance probability; c) CO_2 concentration at 2 m above the ground corresponding to the 5% exceedance probability; d) CO_2 concentration at 2 m above the ground corresponding to the 1% exceedance probability. DEM retrieved from TINITALY/01 dataset (Tarquini et al. 2007).

Figure 6 shows several interesting aspects of the simulated process. The most evident one is the density stratification, with the outputs at 0.05 m above the ground showing significantly higher values of CO_2 concentration. For low exceedance probabilities (e.g. 1%) values above 10,000 ppm averaged over the whole simulation duration (2 hours) affect most of the valley, particularly towards the east close to the source, with local peak values around 120,000 ppm, which agree with Chiodini et al. [2010] measurements. The E-W trending valley and the source area are the most hazardous zones. The probabilistic outputs also show that the possibility for the gas flow not flowing downhill into the valley (e.g. the gas expanding uphill in the tributaries valleys) should not be discarded; this may happen in the case of strong winds.

4. Discussion

The two application examples here presented show some of the potential of VIGIL. The software can in fact be used to generate hazard maps of volcanic gas exploring the meteorological variability as the first controlling factor. The variability of other parameters characterizing the gas emission source like the number of sources, their location and emission rate can also be considered. In this case, for each of the simulations linked to the meteorological variations (e.g. for each simulation day and time interval), the emission source parameters can vary according to the user requirements as discussed in the Methods section. Therefore, another layer of uncertainty related to the source can be overlapped to the uncertainty of meteorological conditions.

Treating the source parameters uncertainty at the same level as the meteorological variability, i.e. fully combining M simulations each with a specific set of source parameters with the N simulations with varying meteorological conditions is currently not supported and will be introduced in the next development steps. This can be crucial to assess the hazard of volcanic gases in contexts where the source location can change and/or is unknown and the gas emission rates vary and/or are unknown. In contexts of relatively steady degassing, like those discussed in the application example, the current version of VIGIL is suitable to quantify the probabilistic gas hazard and, by exploring the meteorological variability sampling a sufficiently high number of days of reanalysis one can quantify the potential exposure to dangerous levels of volcanic gases concentration on long-term. VIGIL also allows sam-

pling the reanalysis dataset specifying the months from which to sample the data, hence making a seasonal analysis possible. In fact, in some contexts it has been shown how the seasonal wind pattern plays a role in controlling the gas concentration levels [e.g. Granieri et al., 2013].

Recent and ongoing eruptions in the Reykjanes peninsula (Fagradalsfjall, Iceland), Soufriére St. Vincent (St. Vincent and The Grenadines) and Nyiragongo (Democratic Republic of Congo) stressed the importance of monitoring and modelling volcanic gas dispersion and accumulation during an effusive eruption (the case of Fagradalsfjall), during and after an explosive event (the Soufriére case) and possible lake overturns causing limnic eruptions, which is the cause of concern at the Lake Kivu shores close to the Nyiragongo volcano. The latter case represents a potential application of VIGIL for long-term dense gas hazard quantification using TWODEE. Furthermore, the next version of VIGIL will allow to run the complete workflow in forecast mode with the possibility to take the source uncertainty into account.

5. Conclusions

In this paper we presented VIGIL, a set of Python scripts designed to manage the complete workflow from gas dispersion simulations to production and visualization of hazard maps aimed at hazard analyses or sensitivity studies. In fact, VIGIL handles the pre-processing (meteorological data retrieval and processing), processing (actual dispersion simulations) and post-processing (e.g. graphical outputs), with the possibility to perform each step exploiting the multiprocessing capabilities of Python. The latter is a fundamental improvement to conduct PVHA applications, which require numerous simulations to take the variability of input parameters of the dispersion models (e.g. meteorological conditions) into account. Additionally, VIGIL represents a valuable tool for sensitivity analyses and validation studies of hazard simulation tools.

VIGIL is interfaced with DIAGNO to provide the mass-consistent wind field necessary to run two dispersion models, DISGAS and TWODEE.

The full range of functionalities is presented in the User's manual provided in the package.

For the future, we plan to implement in VIGIL also further options, such as:
– the calculation of the gas persistence time above user-defined concentration and exposure time thresholds;
– the implementation of full ensemble mode also for the source uncertainty;
– the overlapping of multiple layers in the graphical outputs produced by *post_process.py*. The current version produces contour plots of gas concentration in the pure computational domain; layers with DEM and other features (e.g. towns, roads, etc.) would significantly improve the value and the information contained in the graphical outputs;
– the possibility to specify the format of the outputs (e.g., netCDF), which are currently saved in Golden Surfer GRD format only;
– the possibility to quantitatively compare outputs with user-provided measurements for the test case under analysis. This can be useful for validation studies.

Fabio Dioguardi et al.

References

Burton, R. R., J. Dudhia, A.M. Gadian, and S. D. Mobbs (2017). The use of a numerical weather prediction model to simulate the release of a dense gas with an application to the Lake Nyos disaster of 1986, Meteorol. Appl., 24, 43-51, https://doi.org/10.1002/met.1603.

Cardellini, C., G. Chiodini, F. Frondini, R. Avino, E. Bagnato, S. Caliro and A. Rosiello (2017). Monitoring diffuse volcanic degassing during volcanic unrests: the case of Campi Flegrei (Italy), Scient. Rep., 7, 1, 1-15.

Chiodini, G., F. Frondini, C. Cardellini, D. Granieri, L. Marini and G. Ventura (2001). CO_2 degassing and energy release at Solfatara volcano, Campi Flegrei, Italy, J. Geophys. Res., Solid Earth, 106, B8, 16213-16221.

Chiodini, G., D. Granieri, R. Avino, S. Caliro, A. Costa, C. Minopoli and G. Vilardo (2010). Non-volcanic CO_2 Earth degassing: Case of Mefite d'Ansanto (southern Apennines), Italy, Geophys. Res. Lett., 37, 11, https://doi.org/10.1029/2010GL042858.

Chiodini, G., S. Caliro, R. Avino, G. Bini, F. Giudicepietro, W. De Cesare et al. (2021). Hydrothermal pressure-temperature control on CO_2 emissions and seismicity at Campi Flegrei (Italy), J. Volcanol. Geotherm. Res., 414, 107245, https://doi.org/10.1016/j.jvolgeores.2021.107245.

Copernicus Climate Change Service (C3S) (2017) ERA5: Fifth generation of ECMWF atmospheric reanalyses of the global climate. Copernicus Climate Change Service Climate Data Store (CDS). https://cds.climate.copernicus.eu/cdsapp#!/home.

Costa, A., G. Macedonio and G. Chiodini (2005). Numerical model of gas dispersion emitted from volcanic sources, Ann. Geophys., 48, 4-5.

Costa, A., G. Chiodini, D. Granieri, A. Folch, R. K. S. Hankin, S. Caliro and C. Cardellini (2008). A shallow-layer model for heavy gas dispersion from natural sources: Application and hazard assessment at Caldara di Manziana, Italy, Geochem. Geophys. Geosyst., 9(3), Q03002, doi:10.1029/2007GC001762.

Costa, A., A. Folch and G. Macedonio (2013). Density-driven transport in the umbrella region of explosive eruptions: effects on tephra dispersion models, Geophys. Res. Lett., 40, 1-5.

Costa, A. and G. Macedonio (2016). DISGAS: a model for passive DISpersion of GAS, Rapporti tecnici INGV, Istituto Nazionale Di Geofisica e Vulcanologia, Italy, 332, 2039e7941.

Cortis, A. and C. M. Oldenburg (2009). Short-range atmospheric dispersion of carbon dioxide, Boundary-layer, Meteorol., 133(1), 17-34.

Cronin, S. J. and D. S. Sharp (2002). Environmental impacts on health from continuous volcanic activity at Yasur (Tanna) and Ambrym, Vanuatu, Intern. J. Environm. Health Res., 12, 2, 109-123.

Douglas, S. G., R. C. Kessler and E. L. Carr (1990). User's guide for the Urban Airshed Model. Volume 3. User's manual for the Diagnostic Wind Model (No. PB-91-131243/XAB), Systems Applications, Inc., San Rafael, CA (USA).

Edmonds, M., J. Grattan and S. Michnowicz (2018). Volcanic gas: silent killers, in Observing the Volcano World: Volcano Crisis Communication, Fearnley, C. J., Bird, D. K., Haynes, K., McGuire, W. J. and G. Jolly (Editors). Springer, Cham.

Folch, A., A. Costa and R. K. Hankin (2007). TWODEE-2: Computer Code and Related Documentation, Project INGV-DPC V5 Diffuse degassing in Italy (2005-2007).

Folch, A., A. Costa and R. K. Hankin (2009). TWODEE-2: a shallow layer model for dense gas dispersion on complex topography, Comput. Geosc., 35, 3, 667-674.

Folch, A., J. Barcons, T. Kozono and A. Costa (2017). High-resolution modelling of atmospheric dispersion of dense gas using TWODEE-2.1: application to the 1986 Lake Nyos limnic eruption, Nat. Haz. Earth. Syst. Sci., 17, 861-879, https://doi.org/10.5194/nhess-17-861-2017.

Granieri, D., A. Costa, G. Macedonio, M. Bisson and G. Chiodini (2013). Carbon dioxide in the urban area of Naples: Contribution and effects of the volcanic source, J. Volcanol. Geotherm. Res., 260, 52-61.

Grattan, J. P. and F. B. Pyatt (1999). Volcanic eruptions dry fogs and the European palaeoenvironmental record: localised phenomena or hemispheric impacts?, Glob. Planet. Change., 21, 1-3, 173-179.

Hankin, R. K. S. and R. E. Britter (1999). Twodee: the Health and Safety Laboratory's shallow layer model for heavy gas dispersion Part 3: Experimental validation (Thorney Island), J. Haz. Mat., 66, 3, 239-261.

International Volcanic Health Hazard Network (IVHHN) (2005). Volcanic Gases and Aerosols Guidelines. https://www.ivhhn.org/images/pdf/gas_guidelines.pdf

Macedonio, G. and A. Costa (2002). Finite element modeling of gas dispersion in the atmosphere, in Proceedings of the Arezzo Seminar in Fluids Geochemistry, Ospedaletto, Italy, 2002.

Magill, C. and R. Blong (2005). Volcanic risk ranking for Auckland, New Zealand. I: Methodology and hazard investigation, Bull. Volcanol. 67, 331-339, https://doi.org/10.1007/s00445-004-0374-6.

Martí, J., W. P. Aspinall, R. Sobradelo, A. Felpeto, A. Geyer, R. Ortiz et al. (2008). A long-term volcanic hazard event tree for Teide-Pico Viejo stratovolcanoes (Tenerife, Canary Islands), J. Volcanol. Geotherm. Res., 178, 543-552, http://dx.doi.org/10.1016/j.jvolgeores.2008.09.023.

Massaro, S., Dioguardi, F., Sandri, L., Tamburello, G., Selva, J., Moune, S., Jessop, D. E., R. Moretti, J. C. Komorowski, and A. Costa (2021). Testing gas dispersion modelling at La Soufrière volcano (Guadeloupe, Lesser Antilles), J. Volcanol. Geotherm. Res, https://doi.org/10.1016/j.jvolgeores.2021.107312.

Massaro, S., F. Dioguardi, M. Stocchi, A. Costa, G. Macedonio, A. Folch, L. Sandri, J. Selva, G. Tamburello and G. Chiodini (2022). A workflow for probabilistic gas dispersion modelling: Examples from Solfarara volcano (Campi Flegrei, Italy), Il Nuovo Cimento, submitted.

Neri, A., W. P. Aspinall, R. Cioni, A. Bertagnini, P. J. Baxter, G. Zuccaro, et al. (2008). Developing an Event Tree for probabilistic hazard and risk assessment at Vesuvius, J. Volcanol. Geotherm. Res., 178, 397-415, https://doi.org/10.1016/j.jvolgeores.2008.05.014

Pedone, M., A. Aiuppa, G. Giudice, F. Grassa, C. Cardellini, G. Chiodini and M. Valenza (2014). Volcanic CO_2 flux measurement at Campi Flegrei by tunable diode laser absorption spectroscopy, Bull. Volcanol., 76, 4, 812.

Pedone, M., D. Granieri, R. Moretti, A. Fedele, C. Troise, R. Somma and G. De Natale (2017). Improved quantification of CO_2 emission at Campi Flegrei by combined Lagrangian Stochastic and Eulerian dispersion modelling, Atm. Environm. 170, 1-11.

Prabha, T. and E. Mursch-Radlgruber (1999). Modeling of diffusion in a wide Alpine Valley, Theor. Appl. Climatol., 64, 93-103.

Sandri, L., J. C. Thouret, R. Constantinescu, A. Biass and R. Tonini (2014). Long-term multi-hazard assessment for El Misti volcano (Peru), Bull. Volcanol. 76, 771, https://doi.org/10.1007/s00445-013-0771-9.

Self, S. (2006). The effects and consequences of very large explosive volcanic eruptions, Phil. Trans. R. Soc. A., 364, 2073-2097, https://doi.org/10.1098/rsta.2006.1814.

Selva, J., A. Costa, W. Marzocchi and L. Sandri (2010). BET_VH: exploring the influence of natural uncertainties on long-term hazard from tephra fallout at Campi Flegrei (Italy), Bull. Volcanol., 72, 717-733, https://doi.org/10.1007/s00445-010-0358-7.

Selva, J., A. Costa, G. De Natale, M. A. Di Vito, R. Isaia and G. Macedonio (2018). Sensitivity test and ensemble hazard assessment for tephra fallout at Campi Flegrei, Italy, J. Volcanol. Geotherm. Res., 351, 1-28, doi:10.1016/j.jvolgeores.2017.11.024.

Selva, J., C. Bonadonna, S. Branca, G. De Astis, S. Gambino, A. Paonita, M. Pistolesi, T. Ricci, R. Sulpizio and A. Ricciardi (2020). Multiple hazards and paths to eruptions: A review of the volcanic system of Volcano (Aeolian Islands, Italy), Earth Sci. Rev., 207, 103186, https://doi.org/10.1016/j.earscirev.2020.103186.

Tarquini, S., I. Isola, M. Favalli and A. Battistini (2007). TINITALY, a digital elevation model of Italy with a 10 meters cell size (Version 1.0) [Data set], Istituto Nazionale di Geofisica e Vulcanologia (INGV), https://doi.org/10.13127/TINITALY/1.0.

Tierz, P., L. Sandri, A. Costa, R. Sulpizio, L. Zaccarelli, M. A. Di Vito and W. Marzocchi (2016). Uncertainty Assessment of Pyroclastic Density Currents at Mount Vesuvius (Italy) Simulated Through the Energy Cone Model, in Natural Hazard Uncertainty Assessment: Modeling and Decision Support, Riley, K., Webley, P. and M. Thompson (Editors). American Geophysical Union.

Williams-Jones, G. and H. Rymer (2015). Hazards of volcanic gases, in The Encyclopedia of Volcanoes, H. Sigurdsson (Editor), Academic Press.

*CORRESPONDING AUTHOR: Fabio DIOGUARDI,
British Geological Survey, The Lyell Centre,
Edinburgh, United Kingdom,
email fabiod@bgs.ac.uk